MTOpen

An Infection-enhanced Oncolytic Adenovirus Secreting *H. pylori* Neutrophil-activating Protein with Therapeutic Effects on Neuroendocrine Tumors

Mohanraj Ramachandran[1], Di Yu[1], Alkwin Wanders[1], Magnus Essand[1] and Fredrik Eriksson[1]

[1]*Department of Immunology, Genetics and Pathology, Uppsala University, Uppsala, Sweden*

Helicobacter pylori neutrophil-activating protein (HP-NAP) is a major virulence factor involved in *H. pylori* infection. HP-NAP can mediate antitumor effects by recruiting neutrophils and inducing Th1-type differentiation in the tumor microenvironment. It therefore holds strong potential as a therapeutic gene. Here, we armed a replication-selective, infection-enhanced adenovirus with secretory HP-NAP, Ad5PTDf35-[Δ24-sNAP], and evaluated its therapeutic efficacy against neuroendocrine tumors. We observed that it could specifically infect and eradicate a wide range of tumor cells lines from different origin *in vitro.* Insertion of secretory HP-NAP did not affect the stability or replicative capacity of the virus and infected tumor cells could efficiently secrete HP-NAP. Intratumoral administration of the virus in nude mice xenografted with neuroendocrine tumors improved median survival. Evidence of biological HP-NAP activity was observed 24 hours after treatment with neutrophil infiltration in tumors and an increase of pro-inflammatory cytokines such as tumor necrosis factor (TNF)-α and MIP2-α in the systemic circulation. Furthermore, evidence of Th1-type immune polarization was observed as a result of increase in IL-12/23 p40 cytokine concentrations 72 hours postvirus administration. Our observations suggest that HP-NAP can serve as a potent immunomodulator in promoting antitumor immune response in the tumor microenvironment and enhance the therapeutic effect of oncolytic adenovirus.

Received 4 April 2013; accepted 24 June 2013; advance online publication 6 August 2013. doi:10.1038/mt.2013.153

INTRODUCTION

Oncolytic viruses have been shown to be promising agents for cancer treatment[1,2] because after administration virus selectively infects and lyses tumor cells where after the released progeny virions reinfect neighboring tumor cells and also enter the blood stream to infect metastasized tumor cells. Oncolytic adenovirus is immunogenic,[3] but is considered to be safe and have been used in several clinical settings.[4,5] Conditionally replicating adenoviruses (CRAds) with a 24 bp deletion in the retinoblastoma protein (pRb)-binding domain of the E1A gene (E1AΔ24) have been shown to have virus replication restricted to cells that have a defective pRb-p16 pathway.[6] As most cancers have a defective pRb-p16 pathway, this virus provides an attractive platform for systemic spread. Many reports have suggested that oncolytic viruses could mount tumor-specific immune response which when combined with oncolysis, may enhance the therapeutic efficacy.[7,8] However the antitumor immune response mounted by adenovirus oncolysis seems to be insufficient to acquire a good therapeutic effect in the clinical setting. This calls for other strategies to improve the antitumor immune response induced by oncolysis. Arming adenoviruses with therapeutic genes coding for immune-modulating proteins seems promising.[9,10] Innate immune cells have been reported to have good antitumor effect[11,12] and induction of innate immune cell infiltration in tumors has been shown to improve the efficacy of oncolytic viruses.[13,14]

Helicobacter pylori neutrophil-activating protein (HP-NAP) is a water-soluble 150 kDa dodecameric protein made up of several identical 15 kDa subunits.[15,16] HP-NAP has been identified as a major virulence factor involved in *H. pylori* infection and promotes neutrophil infiltration to the site of infection.[17,18] It is a toll-like receptor-2 agonist and binds to toll-like receptor-2 on neutrophils via its C-terminal region[19] thus stimulating a cascade of intracellular events like increase in cytosolic Ca^{2+} concentrations, phosphorylation, and assembly of cytosolic subunits of NADPH oxidases, which leads to the production of reactive oxygen intermediates (ROIs).[18] HP-NAP is a potent immunomodulator, capable of inducing secretion of the proinflammatory cytokines tumor necrosis factor (TNF)-α and interleukin (IL)-8[20] and T helper type 1 (Th1) type immune polarization with secretion of IL-12 and IL-23.[21,22] Given the ability of activated neutrophils to eradicate tumors[11,12] and the ability to induce a Th1-type immune polarization,[21,22] we believe that HP-NAP is a potential candidate as a therapeutic gene that can enhance the therapeutic efficacy of oncolytic adenovirus.

The last two authors contributed equally to this work.

Correspondence: *Magnus Essand, Department of Immunology, Genetics and Pathology, Uppsala University, SE-75185 Uppsala, Sweden.*
Email: magnus.essand@igp.uu.se

In this study, we aimed to evaluate the therapeutic potential of the infection-enhanced (capsid- and fiber-modified), replication-selective (E1AΔ24) oncolytic adenovirus serotype-5 (Ad5) armed with soluble HP-NAP as an immunomodulatory gene, Ad5PTDf35-[Δ24-sNAP].

RESULTS

HP-NAP protein is expressed and secreted in its biologically active form

The HP-NAP transgene was placed downstream of the adenovirus E1AΔ24 gene, separated by a self-cleaving T2A peptide. The HP-NAP gene was also equipped with an artificial signal peptide at the N-terminal end, which helps in efficient secretion of the protein (**Figure 1a**). To verify secretion, we performed immunoblots to detect the secreted HP-NAP protein. Supernatants and cell lysates (secretion blocked with Brefeldin A) were harvested from 24-hour culture of neuro-endocrine cells (BON) transduced with Ad5PTDf35-[Δ24-sNAP], Ad5PTDf35-[Δ24] and Ad5PTDf35-[GFP]. We found HP-NAP as a 15 kDa monomer[15,16] secreted from Ad5PTDf35-[Δ24-sNAP]-transduced cells and in the cell lysate when secretion was blocked with Brefeldin A (**Figure 1b**) when using a specific antibody clone 16F4. Cells transduced with the viruses lacking HP-NAP did not show any corresponding protein band in the immunoblot (**Figure 1b**).

Previous reports have shown that *H. pylori* infection in humans is associated with strong neutrophil infiltration[23,24] suggesting a possible bacterial virulence factor to be involved in inducing chemotaxis. Studies with purified HP-NAP protein have shown that it is chemotactic for neutrophils and monocytes in a concentration-dependent manner.[18] A transwell migration assay of neutrophils against supernatants from virus-transduced cells was performed to assess chemotactic ability. It was observed that there is significant neutrophil chemotaxis towards Ad5PTDf35-[Δ24-sNAP]-transduced BON cell culture supernatant (Mann–Whitney *U* test, $^{***}P < 0.001$) and not towards Ad5PTDf35-[Δ24]-transduced or untransduced BON cell culture supernatant (**Figure 2a**).

Biologically active HP-NAP protein is known to bind toll-like receptor-2 on neutrophils and stimulate the production of ROIs, which is mediated by activation of NADPH oxidases.[18,25,26] A flow cytometry-based assay was used to detect ROI production of activated human neutrophils in response to stimulation with virus-transduced BON cell supernatant. Dihydro-rhodamine (DHR123) was used as the marker for ROI detection. We noted a significant increase in the levels of ROI production when human neutrophils were activated with supernatant harvested from Ad5PTDf35-[Δ24-sNAP]-transduced BON cell culture (mean fluorescence intensity: 2960) compared with the Ad5PTDf35-[Δ24]-transduced (mean fluorescence intensity: 580) or untransduced (mean fluorescence intensity: 430) BON cell culture supernatant (**Figure 2b**), (Mann–Whitney *U* test, $^{**}P < 0.01$; $^{*}P < 0.05$). This data suggests that oncolytic adenoviruses could be used as a vector to deliver secreted HP-NAP in its biologically active form.

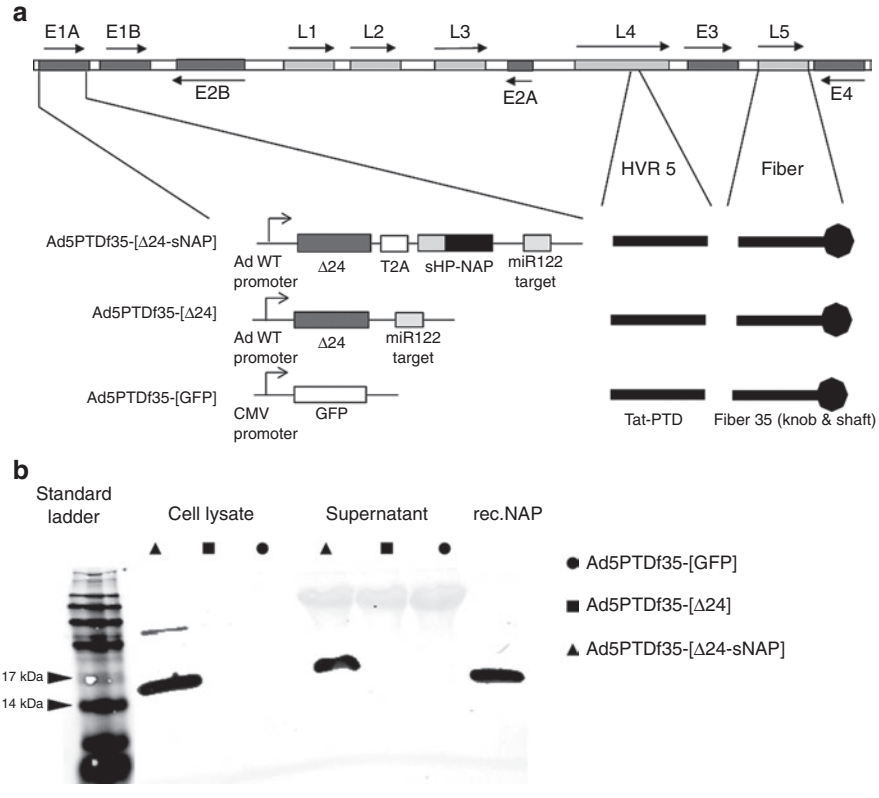

Figure 1 Schematic illustration of viruses used in the experiment and immunoblotting showing production of HP-NAP. (**a**) Ad5PTDf35-[Δ24-sNAP], Ad5PTDf35-[Δ24], and Ad5PTDf35-[GFP]. (**b**) BON cells were transduced with Ad5PTDf35-[Δ24-sNAP], Ad5PTDf35-[Δ24], or Ad5PTDf35-[GFP]. Total cell lysate (where secretion was blocked with Brefeldin A) or supernatant were harvested 24 hours post-transduction and samples were resolved by 10% SDS-PAGE. HP-NAP was detected by immunoblotting using anti-HP-NAP antibody (Clone 16F4). Recombinant HP-NAP protein (50 ng) was used as a positive control.

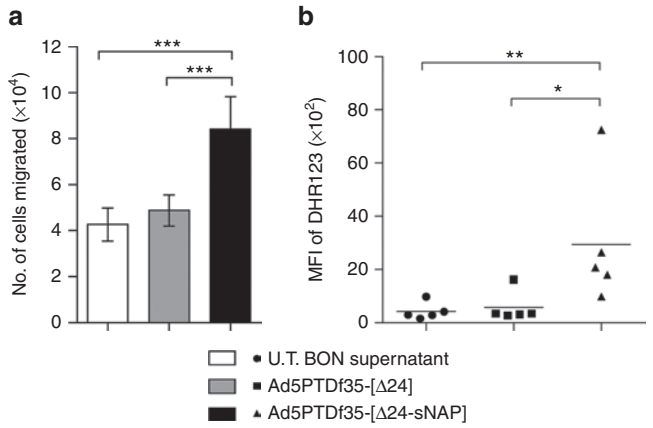

Figure 2 Biological activity of secreted HP-NAP. BON cells were transduced with viruses Ad5PTDf35-[Δ24-sNAP] or Ad5PTDf35-[Δ24] at MOI 10 FFU/cell. Supernatants were harvested 48 hours post-transduction. (**a**) Transwell migration assay of human neutrophils isolated from four different individuals (2×10^5 cells/well) against harvested supernatants for 2 hours at 37 °C. All samples were analyzed in triplicates and the data is represented as mean + SD of number of cells migrated. Supernatant from untransduced (U.T.) BON cells were used as control, (***$P < 0.001$; $n = 12$). (**b**) Granulocyte activation assay with supernatants from virus-transduced BON cells for 30 minutes at 37 °C. Activation was measured in terms of ROI production, which was monitored using fluorescent dye DHR123. Supernatant from untransduced BON cells were used as control. At least 10,000 events were recorded in the flow cytometer and MFI of DHR123 was recorded, (**$P < 0.01$; *$P < 0.05$; $n = 5$). MFI, mean fluorescence intensity.

Oncolytic adenovirus carrying the HP-NAP transgene exhibited improved cell killing in a majority of the tumor cell lines examined

The Ad5 viruses constructed for this study have the serotype-35 fiber and a protein transduction domain (PTD) sequence inserted in hexon hyper variable region 5, hence show enhanced infectivity on a wide range of cell types.[27,28] The Ad5PTDf35-[Δ24-sNAP] and Ad5PTDf35-[Δ24] viruses have the E1A region under the control of the wild-type Ad5 E1A promoter, but the E1A gene has a 24 bp deletion, which confers selectivity of virus replication in pRb pathway-deficient cells.[6,29] Otherwise, the viruses contain wild-type Ad5 sequences. The oncolytic efficacy of Ad5PTDf35-[Δ24-sNAP] was examined on tumor cell lines from different origin. The cell lines were transduced in suspension at various multiplicity of infections (MOIs) ranging from 0.01 to 10 fluorescence forming unit (FFU)/cell and the relative cell viability was measured at day 5 (**Figure 3a–d**). Ad5PTDf35-[Δ24-sNAP] had eradicated more than 95% of BON (**Figure 3a**), 90% of SK-N-FI (**Figure 3b**), 75% of CNDT2.5 (**Figure 3c**) at MOI 10, and 85% of mel526 cells (**Figure 3d**) at MOI 1000. Whereas, Ad5PTDf35-[Δ24] had comparatively lesser killing efficiency compared with HP-NAP armed adenovirus (**Figure 3a–d**). The mock virus did not have any significant killing effect (**Figure 3a–d**). Thus, the insertion of HP-NAP transgene in the adenovirus genome does not negatively affect its oncolytic activity and a moderate, though not statistically significant, increased killing effect was observed.

TNF-α is one of the important cytokines that is triggered upon HP-NAP infection[20] and it is known that TNF-α can have direct therapeutic effect and that it could possibly affect oncolysis as well. We therefore evaluated the effect of tumor cell killing by adenovirus in the presence of TNF-α *in vitro*. We observed that BON cells were killed to similar degrees by viruses when transduced at a high MOI (10 FFU/cell) and cultured with or without addition of 100 ng/ml TNF-α (**Figure 3e**). However, a significant inhibition in tumor growth (>40% after 8 days) was observed when cells were transduced with viruses at a low MOI (0.01 FFU/cell) and cultured with 100 ng/ml TNF-α compared with transduced cells cultured without TNF-α (**Figure 3f**) (Mann–Whitney *U* test, *$P < 0.05$). This suggests that secretion of TNF-α after activation of immune cells by HP-NAP at early stages of adenovirus infection would be beneficial for tumor cell killing.

Arming adenovirus with HP-NAP does not affect vector stability and oncolytic virus spread

Genetic modification of adenoviruses has sometimes led to vector instability and inefficient viral spread. A PCR was done to quantify the number of viral particles in terms of encapsidated viral genome (evg) after a high-titer production of recombinant adenoviruses in 911 cells. We obtained very high titers of all the recombinant adenoviruses constructed (**Table 1**). In particular, we obtained higher titers of Ad5PTDf35-[Δ24-sNAP] (2.1×10^{12} evg/ml) compared with that of Ad5PTDf35-[Δ24] (1.9×10^{10} evg/ml), indicating that the introduction of HP-NAP into adenovirus genome does not negatively affect its genetic stability. We also performed a plaque formation assay to demonstrate the effect of HP-NAP insertion on oncolytic virus spread to neighboring cells during virus replication. The plaques formed by viruses Ad5PTDf35-[Δ24-sNAP] and Ad5PTDf35-[Δ24] were visible by day 10 and both viruses formed plaques of similar sizes. Plaques formed by both viruses on day 14 are shown at 20× magnification with inserted figures at 40× magnification (**Figure 3g**, **h**).

Repeated intratumoral injections of Ad5PTDf35-[Δ24-sNAP] improves survival of nude mice carrying neuroendocrine tumors

To evaluate the therapeutic potential of the oncolytic virus carrying the HP-NAP transgene *in vivo*, female NMRI nude mice xenografted with human neuroendocrine tumor, BON, were used. Once the implanted tumors were palpable on all the mice, they were treated four-times every third day with intratumoral injections of Ad5PTDf35-[Δ24-sNAP] or Ad5PTDf35-[Δ24] or Ad5PTDf35-[GFP] as control. Mice treated with Ad5PTDf35-[Δ24-sNAP] and Ad5PTDf35-[Δ24] showed significant tumor growth suppression (**Figure 4a**) compared with the Ad5PTDf35-[GFP]-treated controls. All the tumors in the control group grew rapidly and all the mice were killed by day 33. The growth of Ad5PTDf35-[Δ24-sNAP] and Ad5PTDf35-[Δ24]-treated tumors was arrested initially but showed steady regrowth after day 50. They were then treated once more with an intratumoral injection. Even though mice in the two treatment groups showed equal regrowth over several weeks thereafter, Ad5PTDf35-[Δ24-sNAP]-treated tumors were free from wounds while Ad5PTDf35-[Δ24]-treated tumors were ulcerated and bleeding. All mice in the Ad5PTDf35-[Δ24]-treated group had to be killed by day 104. At day 104 post-tumor inoculation there was a significant difference in the tumor sizes of mice treated with Ad5PTDf35-[Δ24-sNAP]

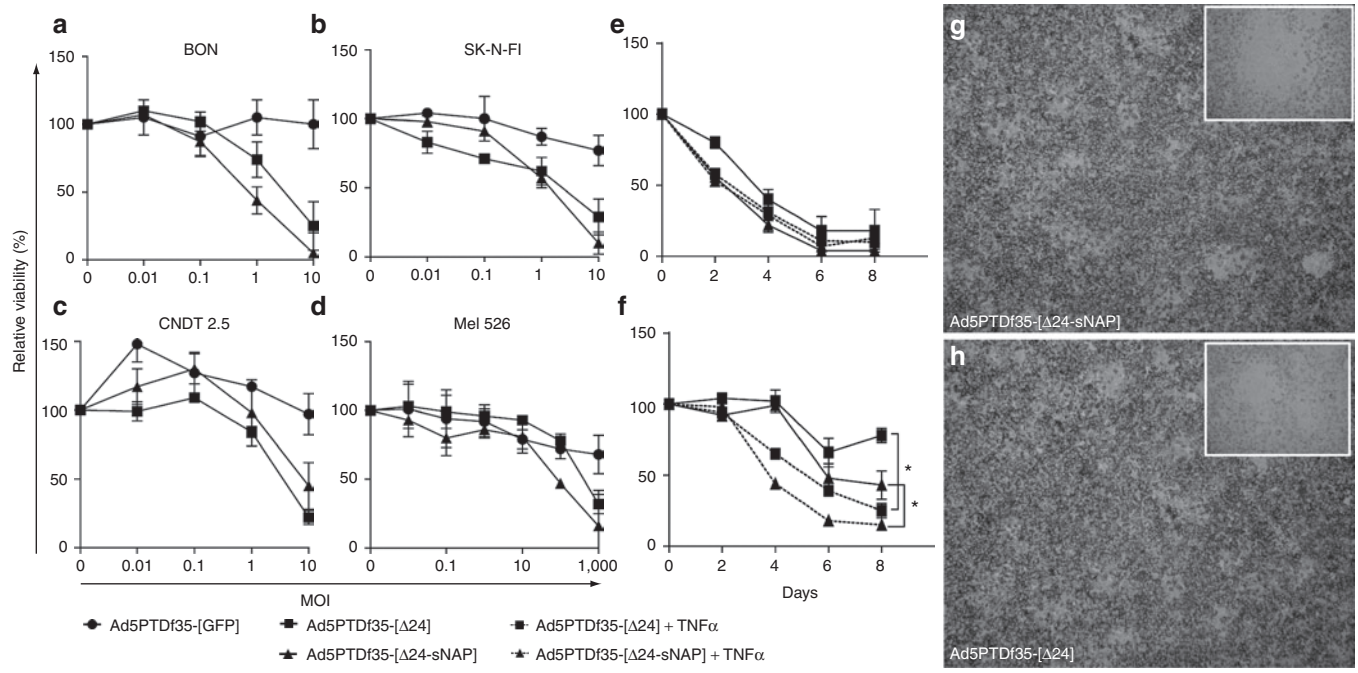

Figure 3 *In vitro* **antitumor activity and plaque formation assay of constructed viruses on tumor cell lines.** Cells of various origin (**a, c**) neuroendocrine tumor cell lines BON and CNDT2.5, (**b**) human neuroblastoma cell line SK-N-FI and (**d**) human melanoma cell line mel526 were transduced with Ad5PTDf35-[Δ24-sNAP], Ad5PTDf35-[Δ24], or Ad5PTDf35-[GFP] at various MOIs ranging from 0.01 to 1,000 FFU/cell in suspension for 2 hours and plated in a 96-well plate (10,000 cells/well). Cell viability was examined 5 days post-transduction by MTS assay. (**e, f**) Neuroendocrine tumor cell line BON transduced with Ad5PTDf35-[Δ24-sNAP], Ad5PTDf35-[Δ24] at MOIs 10 (**e**) and 0.01 (**f**), plated in a 96-well plate (10,000 cells/well) and cultured with or without 100 ng/ml TNF-α. Cell viability was measured at 2, 4, 6, and 8 days post-transduction. Values represent viability in relation to untransduced cells. Average values + SD from triplicate samples are shown (*$P < 0.05$). (**g, h**) A549 cells transduced with either Ad5PTDf35-[Δ24-sNAP], or Ad5PTDf35-[Δ24] respectively and overlayed with culture medium mixed with low-melting point agar (1:1 v/v) containing neutral red to visualize plaques. Pictures were taken after 14 days at 200× original magnification with in folded pictures at 400× original magnification.

Table 1 FFU and evg values for different adenovirus vectors produced

Vector	FFU/ml	evg/ml	evg/FFU
Ad5PTDf35-[GFP]	6.9×10^{10}	4.5×10^{11}	6.5
Ad5PTDf35-[Δ24]	2.0×10^{09}	1.9×10^{10}	9.5
Ad5PTDf35-[Δ24-sNAP]	1.5×10^{11}	2.1×10^{12}	14

evg, encapsidated viral genome; FFU, fluorescence forming unit.

(Mann–Whitney *U* test, ***$P < 0.001$) compared with mice treated with Ad5PTDf35-[Δ24] virus. Ad5PTDf35-[Δ24-sNAP]-treated mice also had a significantly prolonged survival with a median survival of 104 days compared with Ad5PTDf35-[Δ24] with a median survival of 76 days (Log-rank (Mantel-Cox) test, **$P <$ 0.01) (**Figure 4b**). The experiment was stopped on day 150, since the mice that had survived did not show any change in tumor volume over the final 3 weeks. Histological analysis of tumor tissues isolated from Ad5PTDf35-[Δ24]-treated mice that were killed at day 104 revealed that the tissues contained actively proliferating tumor cells with about 40% tumor necrosis and that the tumor is rather large (**Figure 4c**).Whereas, histological analysis of the tissues isolated from the two survivors of Ad5PTDf35-[Δ24-sNAP]-treated mice on day 150 revealed that, one of the remaining tissue contained a small tumor nodule (max. 2 mm in size) with more than 60% tumor necrosis (**Figure 4d**) and the other tissue contained a small regular structured lymph node surrounded by fat without any sign of tumor growth or metastasis (**Figure 4e**). This data suggests that treatment with Ad5PTDf35-[Δ24-sNAP] prolongs survival of nude mice bearing neuroendocrine tumors.

Treatment with Ad5PTDf35-[Δ24-sNAP] induces proinflammatory and Th1-type cytokines *in vivo*

To investigate the role of HP-NAP in contributing towards the antitumor effect that could act additively or synergistically with the oncolytic activity, we treated mice-bearing subcutaneous BON tumors with intratumoral injections of Ad5PTDf35-[Δ24-sNAP] or Ad5PTDf35-[Δ24] twice, on day 10 and 12 after tumor implantation (**Figure 5a**, T1 and T2), and two mice per group were killed 1 or 2 days after treatment (**Figure 5a**, T1-D1, T2-D1 and T2-D2). Plasma and tumor samples were collected and analyzed for proinflammatory and Th1-type cytokines by ELISA. Untreated tumor-bearing mice were used as control. A delayed upregulation of TNF-α in the tumor mass was observed in the mice treated with Ad5PTDf35-[Δ24-sNAP] (on T2-D2 mean: 2.5 ng/g tumor mass) when compared with the group of Ad5PTDf35-[Δ24]-treated mice (**Figure 5b**). Although there was a tendency of higher TNF-α in the mice treated with Ad5PTDf35-[Δ24-sNAP] at earlier time points we did not observe significant difference in TNF-α levels in the tumors between the groups (**Figure 5b**). However, in the plasma samples from Ad5PTDf35-[Δ24-sNAP]-treated mice we observed an increase in levels of the proinflammatory cytokines TNF-α and MIP2-α and the Th1 cytokine IL-12/23 p40 from

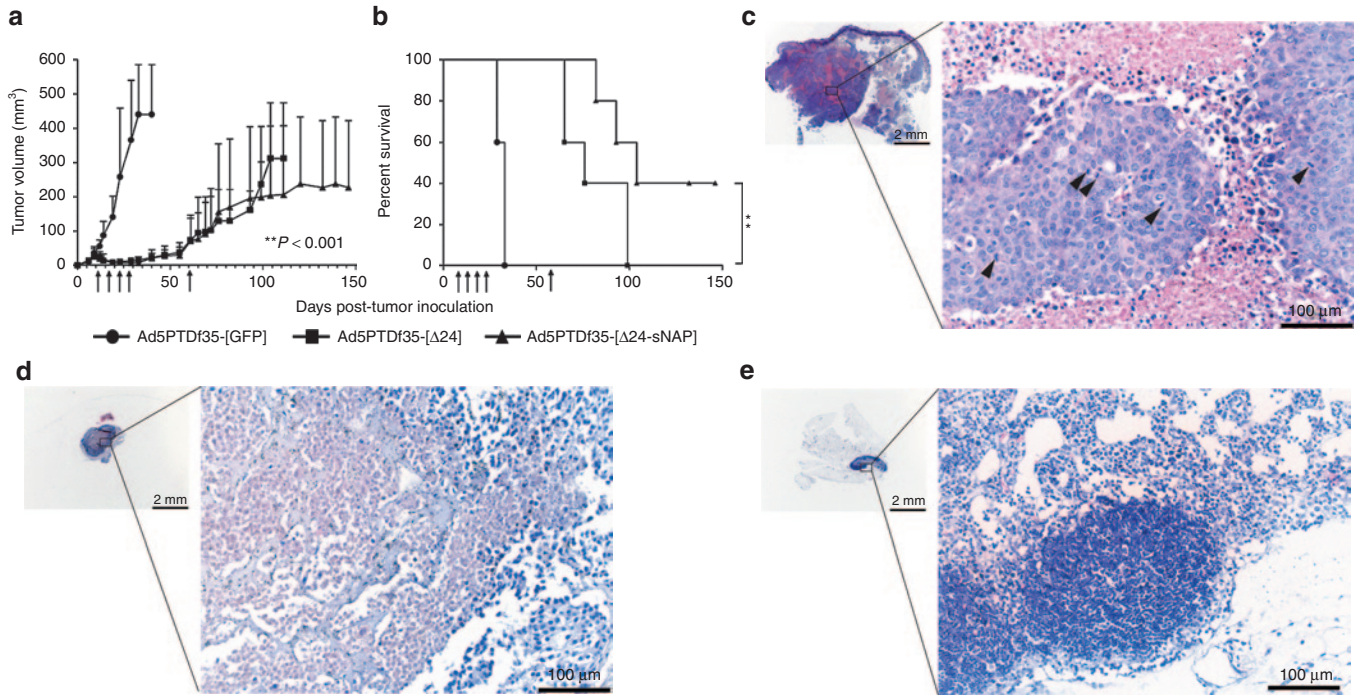

Figure 4 Ad5PTDf35-[Δ24-sNAP] prolongs survival of NMRI nude mice-bearing neuroendocrine tumor. BON (5×10^6 cells) were injected s.c. in nude mice. The mice were treated with Ad5PTDf35-[Δ24-sNAP], Ad5PTDf35-[Δ24], or Ad5PTDf35-[GFP] (5×10^8 FFU/injection) at time points as indicated by arrows in the figures. Tumor growth was monitored by caliper measurements. (**a**) Tumor size curve for mice treated with different virus is shown. Values represent mean tumor volume (mm^3) + SD (five mice per group). Mice were killed when tumor volume reached 800 mm^3 or if the tumors were ulcerated and wounded. Experiment was terminated 150 days post-tumor inoculation because no change in tumor volume was noticed during the final 3 weeks before termination of the experiment. Significant difference in tumor volume in Ad5PTDf35-[Δ24-sNAP]-treated mice was noted after day 104 (***$P < 0.001$; $n = 5$) (**b**) A Kaplan–Meier survival plot shows the survival data and the data were compared by performing a log-rank test (**$P < 0.01$; $n = 5$). (**c**) Representative pictures of histological H&E stained sections of the embedded tumor tissue isolated from Ad5PTDf35-[Δ24]-treated mice on day 104 (mitotic cells are marked by arrows). Original magnification, left panel ×12.5, right panel ×200; scale bar: left panel 2 mm, right panel 100 µm. (**d, e**) Representative pictures of histological H&E stained sections of the embedded tissues isolated from the two survivors of Ad5PTDf35-[Δ24-sNAP]-treated mice when the nongrowing tumors were resected on day 146. Original magnification, left panel ×12.5, right panel ×200; scale bar: left panel 2 mm, right panel 100 µm.

24 hours post treatment (Figure 5c–e). In samples obtained from Ad5PTDf35-[Δ24-sNAP]-treated mice, the concentration of TNF-α was more than two-fold higher on T1-D1 (mean: 187 pg/ml), T2-D1 (mean: 187 pg/ml), and T2-D2 (mean: 145 pg/ml) compared with samples from Ad5PTDf35-[Δ24]-treated mice, (Figure 5c). TNF-α concentration in plasma of untreated mice was 55 pg/ml. Similarly, we observed an immediate increase in the levels of neutrophilic chemo-attractant MIP2-α in Ad5PTDf35-[Δ24-sNAP]-treated mice 1 day after treatment, T1-D1 (mean: 204 pg/ml) and T2-D1 (mean: 300 pg/ml), but decreased to background level 2 days after treatment, T2-D2 (mean: 89 pg/ml) (Figure 5d). MIP2-α concentration in plasma of untreated mice was 53 pg/ml. On the other hand, we noted a significant increase in concentration IL-12/23 p40 in Ad5PTDf35-[Δ24-sNAP]-treated mice only after the second treatment, T2-D1 (mean: 741 pg/ml) and T2-D2 (mean: 830 pg/ml) when compared with samples from Ad5PTDf35-[Δ24] or untreated mice (Figure 5e). IL-12/23 p40 concentration in plasma of untreated mice was 121 pg/ml (Two-way ANOVA, Bonferroni post-test, ***$P < 0.001$;** $P < 0.01$; *$P < 0.05$).

These data suggest that mice treated with Ad5PTDf35-[Δ24-sNAP] virus expresses the HP-NAP transgene *in vivo,* which contributes to the elevated levels of TNF-α both in the plasma and the tumor and other cytokines like MIP2-α immediately after treatment and the Th1 cytokine IL-12/23 p40 three days after the first treatment, which could contribute to the second wave of inflammation at the tumor site.

Ad5PTDf35-[Δ24-sNAP] treatment induces neutrophil migration and tumor necrosis *in vivo*

The tumor samples that were collected at different time points after treatment with viruses, as illustrated in Figure 5a, were analyzed by immunofluorescence and histology. Immunofluorescence of tumor tissue sections with the mouse myeloid differentiation marker Gr1/Ly6 (Alexa-647 conjugated) and the neutrophil-specific enzyme myeloperoxidase (MPO) (stained with streptavidin Alexa-488) revealed the presence of a significantly higher number of double-positive infiltrating polymorphonuclear neutrophils (PMNs) in the Ad5PTDf35-[Δ24-sNAP]-treated tumors compared with other treatment groups. Immunofluorescence staining of tumor sections after treatment with different viruses on T2-D1 is shown at 200× original magnification (Figure 6a–i) where blue spots (Hoechst 33342) show the staining of nuclei. Red spots show the staining for Gr1 (Figure 6a–c), green spots show the staining for MPO (Figure 6d–f) and Gr1/MPO double-positive neutrophilic cells are shown as whitish spots

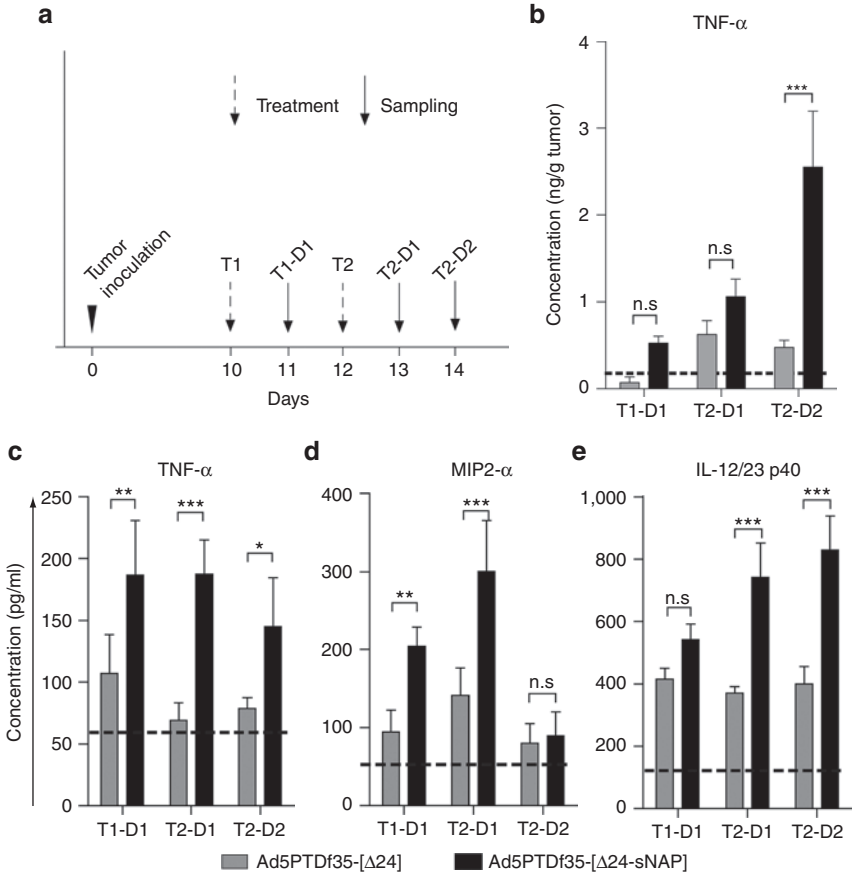

Figure 5 Proinflammatory and Th1-type cytokine levels in tumor and plasma of mice after therapy with HP-NAP-armed adenovirus. (**a**) Mice bearing BON tumors were treated with two intratumoral injections of Ad5PTDf35-[Δ24-sNAP] or Ad5PTDf35-[Δ24] (indicated by dotted arrows) and two mice per group were killed, blood and tumor samples were drawn at different time points (indicated by solid arrows). Cell lysate was prepared by homogenizing frozen tumor samples in 1× TBS with protease inhibitors. Plasma was separated from blood by centrifugation at 300*g* for 10 minutes. Concentration of various cytokines determined by ELISA are represented in (**b**) TNF-α in tumor lysate, (**c**) TNF-α in plasma (**d**) MIP2-α in plasma and (**e**) IL-12/23 p40 in plasma. The dotted lines represent cytokine levels in the tumor lysate and plasma of untreated tumor-bearing mice. All samples were analyzed in duplicates. Data represent mean concentration + SD, (***$P < 0.001$; **$P < 0.01$; *$P < 0.05$; $n = 4$).

in **Figure 6g–i**. The number of infiltrating neutrophils ($Gr1^+/MPO^+$)was significantly higher in Ad5PTDf35-[Δ24-sNAP]-treated tumors than in Ad5PTDf35-[Δ24]-treated tumors (three-fold higher on all days), (**Figure 6m**). Neutrophils are known for nonspecific tissue destruction at the site of infiltration and this was confirmed by histological analysis of the tumor sections with H&E staining (**Figure 6j–l**),which revealed the presence of necrotic areas (encircled with dotted lines). Histological H&E staining of tumor sections after treatment with different viruses on T2-D1 are shown at 100× original magnification (**Figure 6j–l**). An experienced pathologist assessed the percentage of necrosis in relation to the tumor tissue in a blinded manner using a semi-quantitative approach with a scale defined in 10% steps. Tumors treated with Ad5PTDf35-[Δ24-sNAP] exhibited significantly larger areas of necrosis (T2-D1 62% necrosis and T2-D2 54% necrosis) than tumors treated with Ad5f35PTD-[Δ24] (T2-D1 28% necrosis and T2-D2 22% necrosis), (Two-way ANOVA, Bonferroni post-test, *$P < 0.05$),(**Figure 6n**). In conclusion, the data show that treatment with Ad5PTDf35-[Δ24-sNAP] induces neutrophil infiltration and subsequent necrosis in large areas of the tumor.

DISCUSSION

Adenoviruses have been widely used as oncolytic agents and as vehicles for transgene delivery. They can also be modified for controlled replication and enhanced host-cell infectivity, which have made one of the most promising agents for cancer therapy in the clinic. However, limited success has been reported in treatment of advanced cancers when relying on the oncolytic effect alone. Several studies have explored oncolytic adenovirus armed with transgenes to improve their therapeutic effect, *e.g.*, with immune-modulating cytokines and chemokines like GM-CSF,[10] or antiangiogenic approaches with transgenes for antibodies against VEGF receptors.[30]

We hypothesized that adenoviruses armed with the bacterial protein HP-NAP as an immune-modulating agent could significantly enhance the potency of oncolytic adenoviral therapy. It has been shown that the HP-NAP protein is immunogenic and capable of recruiting and activating neutrophils and other immune cells.[18,20,26] Recombinant HP-NAP[31] as well as HP-NAP transgene in an oncolytic vector[32] has shown good therapeutic potential *in vivo*. To achieve this, we inserted a codon-optimized transgene encoding the bacterial HP-NAP protein under the control of

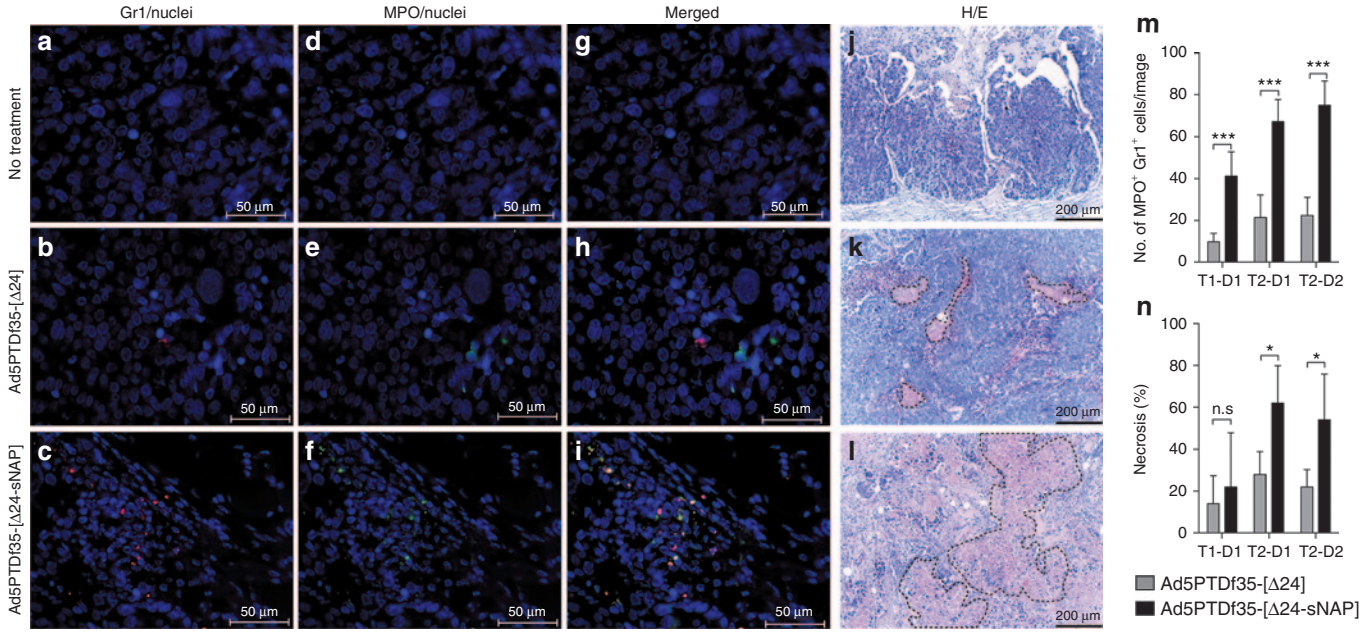

Figure 6 Neutrophil infiltration and necrosis of tumor areas in mice after therapy with HP-NAP-armed adenovirus. Mice-bearing BON tumors were treated with two intratumoral injections of Ad5PTDf35-[Δ24-sNAP] or Ad5PTDf35-[Δ24] and two mice per group were killed, tumor samples were drawn at different time points as illustrated in **Figure 5a**. Immunofluorescence staining of paraffin-embedded tumor tissue sections after the following **(a, d, g)** no treatment (original magnification ×400; scale bar: 50 μm), (**b, e, h**) treatment withAd5PTDf35-[Δ24] (original magnification ×400; scale bar: 50 μm) and (**c, f, i**) treatment with Ad5PTDf35-[Δ24-sNAP] on T2-D1 (original magnification ×400; scale bar 50 μm). The staining was performed with the myeloid differentiation marker Alexa-647-α-Gr1, the neutrophil-specific enzymeAlexa-488-α-MPO and nuclear stain Hoechst 33342. Sections with embedded tumor tissues were also histologically stained using H&E and representative pictures of stained sections after (**j**) no treatment, (**k**) treatment with Ad5PTDf35-[Δ24] and (**l**) treatment with Ad5PTDf35-[Δ24-sNAP] on T2-D1 are shown (original magnification ×100; scale bar: 200 μm). Examples of necrotic areas are encircled with dotted lines. (**m**) The number of $Gr1^+/MPO^+$ cells in tumor/image at 200× original magnification after treatment with virus at different time points. The data represent mean + SD (***$P < 0.001$; $n = 5$). (**n**) Quantitative analysis of percentage of necrosis in the H/E-stained tumor sections after treatment with viruses at different time points. The data represent mean + SD (n.s.: no significance; *$P < 0.05$; $n = 5$).

wild-type E1A promoter behind the E1A gene with a 24 bp deletion in the pRb-binding domain, which confers the specificity of the virus to only replicate in tumor cells.[6,29] The double-modified virus Ad-PTDf35, where the serotype-5 fiber is replaced with the serotype-35 fiber and the HVR5 on the hexon is modified with a cell penetrating peptide, Tat-PTD from HIV-1, was used for this study. This virus has improved transduction on a variety of tumor cell types, including coxsackie-adenovirus receptor-negative tumor cells,[27] and thus confers the ability to treat an array of cancer types with one virus and as well as to transduce primary cells like macrophages, dendritic cells and mesenchymal stem cells,[28] so that these cells can use used as carriers for systemic delivery of virus to prevent clearance of virus by the immune system.[33–35] The E1AΔ24-containing viruses also contains six copies of a target sequence for the liver cell-specific microRNA miR122 in the 3′ untranslated region of the E1A mRNA sequence, to prevent E1AΔ24 protein expression and thereby virus replication in hepatocytes (**Figure 1a**). We and others have previously shown that insertion of miR122 target sequences reduces liver toxicity in mice[36–38] that improves the safety and provides us with an opportunity to increase dosage of virus to be administered.

In vitro, the Ad5PTDf35-[Δ24-sNAP] virus was found to be equally potent as the same virus without transgene in tumor killing assays. In addition it was chemotactic for neutrophils and induced activation of immune cells (**Figure 2a**,**b**), corroborate with previous studies.[18,21] HP-NAP is a potent chemo-attractant for PMN leukocytes only when secreted from the infected cells and can reach the endothelial barrier to stimulate neutrophils.[39] Our studies show that the HP-NAP protein could be expressed and secreted in its biologically active form by tumor cells transduced with our recombinant adenovirus.

Neutrophils are effectors of the innate immune system and are one of the first cell types to enter the site of infection to fight against invading pathogens. They are potential mediators of inflammation and secrete proinflammatory cytokines to recruit other subsets of immune cells.[40] Usually, neutrophilic infiltration is nonspecific and can cause random killing of cells around the site of infection and cause necrosis. This random killing by activated PMNs is mediated by release of reactive oxidants like O^{2-}, H_2O_2, hypochlorous acid and also by granule enzymes like myeloperoxidase and metalloproteinase.[41] TNF-α is one of the important cytokines induced by HP-NAP activation of the immune system. It has been shown to prime PMNs to produce enhanced levels of ROIs induced by HP-NAP.[18] It has been reported that E1A gene expression in cells can sensitize them to TNF-α exposure, which is thought to act through several different mechanisms.[42] In support to this, we have also observed that TNF-α can be beneficial for tumor cell killing at early stages of virus infection (**Figure 3f**). This suggests that the effect of HP-NAP and cytokines may play an important part in amplifying the killing effect by PMNs. HP-NAP

protein by itself does not activate endothelial cells in up regulating adhesion molecules like VCAM-1, ICAM-1, and E-selectin[43] while TNF-α is known to activate endothelial cells to produce adhesion molecules and also IL-8 to promote PMN trans-endothelial migration.[44,45] MIP2-α is the analog to IL-8 in mice, and it is an important chemokine involved in promoting PMN chemotaxis.[44] We detected elevated systemic levels of the proinflammatory cytokines TNF-α and MIP2-α 24 hours after treatment and the Th1-type cytokines IL-12/23 p40 48 hours after treatment with Ad5PTDf35-[Δ24-sNAP] (**Figure 5b–c**), which suggests activation of endothelial and immune cells. HP-NAP is potent in inducing Th1-type immune polarization[31] and suppressing Th2-type immune polarization.[46] They are also known to enhance infiltration of $CD4^+$ and $CD8^+$ IFN-γ secreting T lymphocytes within the tumor microenvironment.[31]

Since HP-NAP plays a key role in activating different immune cell types and stimulating secretion of plethora of cytokines, we wanted to measure systemic level of HP-NAP secreted after virus administration. However, there is unfortunately no commercially available anti-HP-NAP antibody to test this using ELISA. It shall be stressed that we did not observe any macroscopic side effects on the animals treated with Ad5PTDf35-[Δ24-sNAP]. Furthermore, a previous study with recombinant HP-NAP protein treatment of bladder cancer in mice did not find any macroscopic effects in the urine, not even with a dose as high as 50 µg HP-NAP per injection,[31] which is most likely much more than what can be achieved with Ad5PTDf35-[Δ24-sNAP] treatment.

Human adenoviruses do not replicate efficiently in mouse cells, so we opted to test our oncolytic agents on xenografts of human neuroendocrine tumors in an immune-compromised mouse model. In the NMRI nude mouse model, which has a functional innate immune system, but lacks functional T-cell immunity, the Ad5PTDf35-[Δ24-sNAP] virus could prolong survival of mice-bearing neuroendocrine tumor compared with virus lacking the HP-NAP transgene (**Figure 4b**). The tumor volume curves for the treatment groups with Ad5PTDf35-[Δ24-sNAP] and Ad5PTDf35-[Δ24] followed the same trend for most of the experiment. However, treatment with Ad5PTDf35-[Δ24-sNAP] virus induced neutrophil infiltration to the tumor site and caused tumor necrosis. We also observed, a very small dormant and highly necrotic tumor nodule on one of the survivors from the Ad5PTDf35-[Δ24-sNAP]-treated group (**Figure 4d**) and no sign of tumor tissue remaining on the other survivor from the same group (**Figure 4e**). Furthermore, we observed high levels if TNF-α in the tumor microenvironment (**Figure 5b**) in the group of Ad5PTDf35-[Δ24-sNAP]-treated mice and we also showed that TNF-α can have a beneficial effect in combination with viral oncolysis to improve tumor cell killing (**Figure 3f**). Hence, we observe improved tumor killing and more tumor necrosis as a result of arming an oncolytic adenovirus with HP-NAP. It also has been shown by others that treatment of tumors with purified HP-NAP protein also induced necrosis and reduced vascularization in the tumor microenvironment indicating that it is also antiangiogenic.[31]

In the present study we intended to study the ability of HP-NAP to induce an innate immune response, including neutrophil and monocyte infiltration which, in an immune competent host, would bridge way for an adaptive antitumor immune response. We have shown that the acute innate immune response raised by HP-NAP is happening as early as on day 2 after virus injection (**Figure 5**), suggesting the potential activation of Th1-type T-cell response before an antibody response can be raised against HP-NAP. Based on findings by Iankov *et al.*, the anti-HP-NAP antibody titer is expected to peak 4 weeks after immunization.[20] However, in order to study the effects of HP-NAP in the presence of adaptive immunity we are currently developing a system where this virus can be evaluated in an immune competent murine tumor model. In such situation, we expect to see antigen-specific T-cell infiltration, which is predominantly Th1 and Tc1-type, which can synergistically combine its cytotoxic effect with the infiltrating innate immune cells.[31] Cytotoxic T cells also tend to secrete high levels of IFN-γ, which could exert a strong antiangiogenic activity. In such a situation we would expect to have tumor eradication and induction of immunological memory would prevent tumor relapse.

In summary, this study describes that treatment with oncolytic adenovirus armed with HP-NAP has the potential to prolong the survival of tumor-bearing mice. Furthermore, as demonstrated by tumor infiltrating neutrophils and induction of Th1-cytokines, HP-NAP is a potent immunomodulating agent that polarizes the otherwise immunosuppressive tumor microenvironment in favor of antitumor immunity to occur even in the absence of adaptive immunity. Tumor treatment with HP-NAP-secreting adenovirus thus offers a promising novel treatment for solid tumors.

MATERIALS AND METHODS

Cell lines and cell culture. The human neuroendocrine tumor cell lines: BON was obtained from J.C. Thompson and C.M. Townsend, Galveston, TX and CNDT2.5 cell line was obtained from L.M. Ellis, M.D. Anderson, Houston, TX. The human neuroblastoma cell line SK-N-FI and the lung cancer cell line A549 were purchased from ATCC, Rockville, MD and the human melanoma cell line mel526 was obtained from T. Boon, LICR, Belgium. BON was cultured in DMEM Glutamax-I and F-12 Nutrient mixture (Kaighn's modification) at 1:1 ratio, supplemented with 10% fetal bovine plasma (FBS), 1 mmol/l sodium pyruvate and 1% penicillin/streptomycin. CNDT2.5 was cultured in DMEM/F-12 medium, supplemented with 10% FBS, 1% nonessential amino acids, 1 mmol/l vitamins, 3.2 mmol/l L-glutamine, 1 mmol/l sodium pyruvate, 1% penicillin/streptomycin. SK-N-FI and A549 were cultured in DMEM Glutamax-I supplemented with 10% FBS, 1 mmol/l sodium pyruvate, 1% nonessential amino acids and 1% penicillin/streptomycin. Mel526 was cultured in Iscove's modified Dulbecco's medium supplemented with 10% FBS, 3.2 mmol/l L-glutamine and 1% penicillin/streptomycin. All cell cultures were maintained in 95% humidity with 5% CO_2 at 37 °C. All the culture reagents were purchased from Invitrogen (Carlsbad, CA).

Recombinant adenoviral vectors. Recombinant viruses were produced by using the AdEasy system. The pShuttle-Δ24-miR122 was constructed by sub cloning the E1A-Δ24 PCR-amplified sequence from pAd5PTD-(Δ24)[27] into pShuttle (kindly donated by Dr. B. Vogelstein, Johns Hopkins, Baltimore, MD) using the restriction sites XhoI and SalI. The primers used for the PCR were 5′-ctcgagtttgtctagggccgcggggac as forward and 5′-gtcgacacacatttcagtacctcaatctg as reverse primer. The synthetic HP-NAP transgene sequence codon-optimized for *Homo sapiens* was obtained from GenScript (Piscataway, NJ). The transgene contains the last 198 bp of the adenovirus E1A gene, a sequence encoding T2A, which is a self-cleaving peptide derived from *Thosea asigna* virus, an artificial signal peptide,[47] 6× His tag, and the transgene for HP-NAP flanked by HpaI and XbaI restriction sites. It was subcloned into pShuttle-Δ24-miR122,

to construct pShuttle-Δ24-sNAP-miR122.The adenovirus genomes for Ad5PTDf35-[Δ24] and Ad5PTDf35-[Δ24-sNAP] (**Figure 1a**) were obtained through homologous recombination in BJ5183 bacteria between the either of the shuttle plasmids and the Ad5 backbone plasmid pAdEasy (Ad5PTDf35-E3). The produced Ad5 viruses will have two surface modifications; the Ad5 fiber will be replaced with the fiber from serotype-35 and the hexon proteins of the virus capsid will contain a cell penetrating peptide, the protein transduction domain (PTD) from the HIV-1 Tat protein for improved infectivity.[48] The viruses contain the intact E1B gene. The Ad5PTDf35-[GFP] mock virus is aE1A- and E1B-deleted, green fluorescence protein (GFP)-expressing virus modified in fiber and hexon as the other viruses. High titer recombinant adenoviruses were produced in 911 cells by several rounds of amplification, purified by CsCl gradient ultracentrifugation at 25,000 rpm at 4 °C for 2 hours and dialyzed against a dialysis buffer (10 mmol/l Tris-HCl (pH 7.9), 2 mmol/l $MgCl_2$, and 4% w/v sucrose). Virus titers were determined as evg by quantitative PCR[27] and by a FFU assay.[49] Viruses were stored in aliquots at −80 °C.

Immunoblotting for detection of HP-NAP from the transgene. BON cells were transduced in suspension with viruses Ad5PTDf35-[Δ24-sNAP], Ad5PTDf35-[Δ24], and Ad5PTDf35-[GFP] at MOI 10 FFU/cell for 2 hours and plated in six-well plates. Protein secretion was blocked with 25 µg Brefeldin A (Sigma–Aldrich) for one set of transduced cells. Cells were lysed using 1× RIPA buffer (Sigma–Aldrich). Supernatants and cell lysates were collected 24 hours post-transduction for immunoblotting analysis. The samples were run on 10% Tris-SDS PAGE gel and transferred to nitrocellulose membrane using Nitrocellulose iBlot gel transfer stacks (Invitrogen) according to manufacturer's instructions. Recombinant HP-NAP protein (50 ng), kindly provided by Dr. I. Iankov, Mayo Clinic, Rochester MN, was loaded as a positive control. The membrane was blocked with 1% BSA in 1× PBS for 1 hour at room temperature (RT) and the secretory HP-NAP protein was detected using a HP-NAP specific monoclonal antibody clone 16F4, kindly provided by Dr. I. Iankov. 16F4 was diluted 1:20 in 1× PBS with 0.5% Tween-20 (1× PBS-T) and the membrane was incubated overnight at 4 °C. A donkey antimouse antibody IRDye 800CW (BD Biosciences, Franklin Lakes, NJ) was used as the secondary antibody and the membranes were scanned in the Odyssey CLx scanner (LI-COR Biosciences, Lincoln, NE).

In vitro *tumor killing assay for recombinant Ad vectors.* The tumor cell lines BON, CNDT2.5, and SK-N-FI cells were transduced in suspension with viruses Ad5PTDf35-[Δ24-sNAP], Ad5PTDf35-[Δ24], and Ad5PTDf35-[GFP] at MOIs 0.01–10 FFU/cell and mel526 cells at MOIs 0.01–1,000 FFU/cell. After 2 hours of transduction, cells were spun down at 1500 rpm for 5 minutes. The pellet was suspended in medium and plated in a 96-well plate at 10,000 cells/well. Cell viability was analyzed after 5 days of culture at 37 °C, 5% CO_2 using 20 µl MTS aqueous cell titer reagent (Promega, Madison, WI), according to the manufacturers instruction.

In a separate experiment BON cells were transduced in suspension with viruses Ad5PTDf35-[Δ24-sNAP] and Ad5PTDf35-[Δ24] at MOIs 0.01 or 10. After 2 hours of transduction, cells were spun down and resuspended in medium with or without 100 ng/ml recombinant TNF-α and plated in a 96-well plate at 10,000 cells/well. Cell viability was analyzed at days 2, 4, 6, and 8 days post-transduction as described above. Relative viability of cells transduced with virus and cultured with or without TNF-α was calculated with respect to untransduced cells cultured with or without TNF-α respectively. The average triplicate samples of virus-transduced cells were compared with the average of untransduced cells.

Plaque formation assay for recombinant Ad vectors. A plaque formation assay as described previously[50] was performed to visualize plaque forming abilities of recombinant Ad vectors. Briefly, A549 monolayer cells in a six-well plate were transduced with Ad5PTDf35-[Δ24-sNAP] and Ad5PTDf35-[Δ24] at 1×10^5 FFU/well for 4 hours at 37 °C. The transduction medium was removed; the cells were washed with 1× PBS and overlayed with culture medium mixed with low-melting point agar (1:1 v/v). At day 6 cells were again overlayed with culture medium mixed with low-melting point agar (1:1 v/v) containing neutral red (Sigma) for visualization of plaques.

Transwell migration assay. The assay was performed using 96-well microplate Chemotaxis chamber (Neuro Probe, Gaithersburg, MD) containing a polycarbonate membrane filter of 5 µm pore size (Neuro Probe). The upper chamber contained neutrophils isolated from four different donors (in triplicates) in RPMI-1640 medium (2×10^5 cells/well) and the lower chamber contained 410 µl of supernatant from virus-transduced BON cells, day 2 after transduction. The cells were allowed to migrate for 2 hours at 37 °C in 5% CO_2. Nonmigrated cells from the upper surface were detached by incubating the membrane with 100 µl of 2 mmol/l EDTA for 30 min at 4 °C. The cells attached to the bottom of the membrane were spun down at 1500 rpm for 5 minutes. The samples were then enumerated for migrated cells using a Burker chamber.

Granulocyte activation assay and flow cytometry. The intracellular fluorescent probe DHR123 (Molecular Probes, Invitrogen) was used for flow cytometric detection of ROIs produced by granulocytes in response to the following stimuli: (i) 100 ng phorbol-12 myristate-13 acetate (PMA) (Sigma–Aldrich), (ii) 100 µl supernatants harvested after two days from Ad5PTDf35-[Δ24-sNAP], Ad5PTDf35-[Δ24], and Ad5PTDf35-[GFP]-transduced BON cells cultured in phenol red free medium. A modified protocol as described by Maurice *et al.*[51] was used. Briefly, 100 µl of heparinized blood was diluted 1:10 with 1× PBS and the erythrocytes were lysed using 4 ml erythrocyte lysing solution (154 mmol/l ammonium chloride and 10 mmol/l potassium bicarbonate) for 10 minutes at RT. The cells were then washed with sterile 1× PBS once and resuspended in 100 µl 1× PBS and incubated in a shaking water bath at 37 °C for 15 minutes with 2.5 µg/ml DHR123. The various stimuli mentioned above were added and incubated for 30 min at 37 °C in a shaking water bath, centrifuged at 1500 rpm for 5 minutes, and the pellet was washed with a 0.5% sodium azide in 1× PBS. Samples were fixed with 1% paraformaldehyde. The samples were recorded in a flow cytometer (FACS Canto II, BD Biosciences) and the fluorescence of DHR123 was measured in the FITC channel. At least 10,000 events were recorded and the granulocytes were gated based on their granularity and size.

Animal models and Ad therapy experiments. For the *in vivo* studies 3–4-weeks old female NMRI nude mice (Harlan Laboratories, Rossdorf, Germany) were used. All mice were housed at the Rudbeck animal facility (Uppsala, Sweden) in individually ventilated cages (five mice per cage). Tumor implantation was performed after 1 week of acclimatization. Exponentially growing BON cells (5×10^6) were mixed 1:1 (vol/vol) with Matrigel (BD Biosciences) in a total volume of 100 µl and injected subcutaneously (s.c.) into the hind flank of NMRI nude mice. Starting at day 6, mice were treated with intratumoral injections of the following viruses: Ad5PTDf35-[Δ24-sNAP], Ad5PTDf35-[Δ24], or Ad5PTDf35-[GFP] (five mice per group) at a dose of 5×10^8 FFU/injection diluted in 1× PBS (total volume of 100 µl). A total of five treatments were administered at 6, 9, 12, 15, and 60 days post-tumor cell implantation. Tumor growth was monitored regularly using an electronic caliper. Tumor size was calculated using the formula (length × width × height × 0.5). Tumor tissues were harvested for histological analysis when the mice were killed.

Cytokine profiles and immunohistochemistry following Ad therapy of xenografts. BON cells (5×10^6) were mixed 1:1 (vol/vol) with Matrigel (BD Biosciences) in a total volume of 100 µl and injected s.c. into the hind flank of NMRI nude mice. Mice were treated with intratumoral injections of Ad5PTDf35-[Δ24-sNAP], Ad5PTDf35-[Δ24] (5×10^8 FFU/injection) twice on day 10 and 12 after tumor implantation. Two mice per group were killed at different time points (1 day after first injection, 1 and 2 days after the second injection); plasma and tumor samples were

collected. Untreated mice bearing tumor were used as controls. Protein samples from tumors were obtained by homogenizing equal amounts of frozen tumor mass (10 mg) in 100 µl 1× TBS with protease inhibitor. The clarified lysate was used to determine TNF-α level in the tumor by sandwich ELISA (BioLegend). Proinflammatory cytokines IL-12/23 p40 (BioLegend, San Diego, CA), TNF-α, (BioLegend), and MIP2-α (Raybiotech,Norcross, GA) in the plasma samples were quantified using ELISA according to the manufacturer's instructions. Tumors were fixed in formalin. Paraffin-embedded 5 µm sections were prepared for immunohistochemical analysis. The sections were deparafinized and hydrated and antigen revival was carried out by heating the slides to 121 °C in antigen revival solution (Vector Laboratories, Inc., Burlingame, CA) and incubating for 20 minutes. The tissue sections were washed in 1× PBS-T for 5 minutes and blocked with 1% FBS in 1× PBS-T for 1 hour at RT. The sections were double-stained overnight at 4 °C in a dark humidified chamber with a primary Alexa-674-conjugated antimouse Gr1 antibody (1:250) (BioLegend) and a primary biotin-conjugated antimouse MPO antibody (1:250) (Abcam, Cambridge, UK). The sections were washed twice with 1× PBS-T and incubated with streptavidin Alexa-488 (Molecular probes, Invitrogen) for 30 minutes at RT to visualize the biotin-conjugated antibody. The sections were then washed twice with 1× PBS-T, stained with Hoechst 33342 stain (Invitrogen) for 15 minutes at RT and mounted with Fluromount-G (Southern Biotech, Birmingham, AL). Slides for histological analysis were prepared by making 6-µm thickness formalin fixed and paraffin-embedded tumor tissue sections and staining them using standard hematoxylin and eosin staining protocol. An experienced pathologist graded blindly the tumor sections for percentage of necrosis (in five different slides for each sample).

Image analysis. The number of infiltrating PMNs (MPO+ Gr1+) was enumerated using CellProfiler (Broad Institute, Cambridge, MA) image analysis software. A customized pipeline was created as described to enumerate the overlapping blobs in the Alexa-488 and Alexa-647 channel. Intensities of speckles of size 15 pixels were enhanced and intensities of speckles of size less than 10 pixels were suppressed in both Alexa-488 and Alexa-647 channels to distinguish the positive signal from background. Primary objects of size from 10–20 pixels and intensities ranging from 0.05 to 1 from the Alexa-488 channel and intensities ranging from 0.005 to 1 from the Alexa-647 channel were identified and highlighted. Overlapping objects (in both channels) from the identified primary objects were enumerated from five different microscopic slides for each sample at 200× original magnification.

Biosafety level and ethics declaration. The Swedish Work Environment Authority has approved the work with genetic modification of the infectious capacity of human adenovirus serotype-5 (ID number 202100–2932 v66a13 (laboratory) and v67a9 (mice)) and genetic modification of replication capacity of human adenovirus serotype 5 (ID number 202100–2932 v66a11 (laboratory) and v67a7 (mice)). All experiments regarding modified adenovirus were conducted under Biosafety level 2. The Uppsala Animal Ethics Committee has approved the animal studies (ID numbers C319/9 and C195/11).

ACKNOWLEDGMENTS

The authors wish to thank Berith Nilsson for technical assistance and Martin Simonsson, Center for Image Analysis, Science for Life Laboratory, Uppsala University for assisting with image analysis using CellProfiler. All authors read and approved the final version of the manuscript. The Swedish Children Cancer Foundation (PROJ10/027), the Swedish Cancer Society (10–0105 and 10–0552), Gunnar Nilsson's Cancer Foundation, the Swedish Research Council (K2013-55X-22191-01-3) and the Marcus and Marianne Wallenberg's Foundation supported this work. The funders has no role in study design, data collection and analysis, decision to publish, or preparation of the manuscript. The authors declared no conflict of interest.

REFERENCES

1. Essand, M (2013). Virotherapy of neuroendocrine tumors. *Neuroendocrinology* **97**: 26–34.
2. Kaufmann, JK and Nettelbeck, DM (2012). Virus chimeras for gene therapy, vaccination, and oncolysis: adenoviruses and beyond. *Trends Mol Med* **18**: 365–376.
3. Cerullo, V, Seiler, MP, Mane, V, Brunetti-Pierri, N, Clarke, C, Bertin, TK *et al.* (2007). Toll-like receptor 9 triggers an innate immune response to helper-dependent adenoviral vectors. *Mol Ther* **15**: 378–385.
4. Immonen, A, Vapalahti, M, Tyynelä, K, Hurskainen, H, Sandmair, A, Vanninen, R *et al.* (2004). AdvHSV-tk gene therapy with intravenous ganciclovir improves survival in human malignant glioma: a randomised, controlled study. *Mol Ther* **10**: 967–972.
5. Khuri, FR, Nemunaitis, J, Ganly, I, Arseneau, J, Tannock, IF, Romel, L *et al.* (2000). a controlled trial of intratumoral ONYX-015, a selectively-replicating adenovirus, in combination with cisplatin and 5-fluorouracil in patients with recurrent head and neck cancer. *Nat Med* ***6***: 879–885.
6. Heise, C, Hermiston, T, Johnson, L, Brooks, G, Sampson-Johannes, A, Williams, A *et al.* (2000). An adenovirus E1A mutant that demonstrates potent and selective systemic anti-tumoral efficacy. *Nat Med* ***6***: 1134–1139.
7. Qiao, J, Wang, H, Kottke, T, Diaz, RM, Willmon, C, Hudacek, A *et al.* (2008). Loading of oncolytic vesicular stomatitis virus onto antigen-specific T cells enhances the efficacy of adoptive T-cell therapy of tumors. *Gene Ther* **15**: 604–616.
8. Qiao, J, Kottke, T, Willmon, C, Galivo, F, Wongthida, P, Diaz, RM *et al.* (2008). Purging metastases in lymphoid organs using a combination of antigen-nonspecific adoptive T cell therapy, oncolytic virotherapy and immunotherapy. *Nat Med* **14**: 37–44.
9. Kurihara, T, Brough, DE, Kovesdi, I and Kufe, DW (2000). Selectivity of a replication-competent adenovirus for human breast carcinoma cells expressing the MUC1 antigen. *J Clin Invest* **106**: 763–771.
10. Cerullo, V, Pesonen, S, Diaconu, I, Escutenaire, S, Arstila, PT, Ugolini, M *et al.* (2010). Oncolytic adenovirus coding for granulocyte macrophage colony-stimulating factor induces antitumoral immunity in cancer patients. *Cancer Res* **70**: 4297–4309.
11. Eriksson, F, Tsagozis, P, Lundberg, K, Parsa, R, Mangsbo, SM, Persson, MA *et al.* (2009). Tumor-specific bacteriophages induce tumor destruction through activation of tumor-associated macrophages. *J Immunol* **182**: 3105–3111.
12. Eriksson, F, Culp, WD, Massey, R, Egevad, L, Garland, D, Persson, MA *et al.* (2007). Tumor specific phage particles promote tumor regression in a mouse melanoma model. *Cancer Immunol Immunother* **56**: 677–687.
13. Grote, D, Cattaneo, R and Fielding, AK (2003). Neutrophils contribute to the measles virus-induced antitumor effect: enhancement by granulocyte macrophage colony-stimulating factor expression. *Cancer Res* **63**: 6463–6468.
14. Urosevic, M, Fujii, K, Calmels, B, Laine, E, Kobert, N, Acres, B *et al.* (2007). Type I IFN innate immune response to adenovirus-mediated IFN-gamma gene transfer contributes to the regression of cutaneous lymphomas. *J Clin Invest* **117**: 2834–2846.
15. Evans, DJ Jr, Evans, DG, Takemura, T, Nakano, H, Lampert, HC, Graham, DY *et al.* (1995). Characterization of a Helicobacter pylori neutrophil-activating protein. *Infect Immun* **63**: 2213–2220.
16. Zanotti, G, Papinutto, E, Dundon, W, Battistutta, R, Seveso, M, Giudice, G *et al.* (2002). Structure of the neutrophil-activating protein from Helicobacter pylori. *J Mol Biol* **323**: 125–130.
17. Choli-Papadopoulou, T, Kottakis, F, Papadopoulos, G and Pendas, S (2011). Helicobacter pylori neutrophil activating protein as target for new drugs against H. pylori inflammation. *World J Gastroenterol* **17**: 2585–2591.
18. Satin, B, Del Giudice, G, Della Bianca, V, Dusi, S, Laudanna, C, Tonello, F *et al.* (2000). The neutrophil-activating protein (HP-NAP) of Helicobacter pylori is a protective antigen and a major virulence factor. *J Exp Med* **191**: 1467–1476.
19. Kottakis, F, Papadopoulos, G, Pappa, EV, Cordopatis, P, Pentas, S and Choli-Papadopoulou, T (2008). Helicobacter pylori neutrophil-activating protein activates neutrophils by its C-terminal region even without dodecamer formation, which is a prerequisite for DNA protection–novel approaches against Helicobacter pylori inflammation. *FEBS J* **275**: 302–317.
20. Iankov, ID, Haralambieva, IH and Galanis, E (2011). Immunogenicity of attenuated measles virus engineered to express Helicobacter pylori neutrophil-activating protein. *Vaccine* **29**: 1710–1720.
21. D'Elios, MM, Amedei, A, Cappon, A, Del Prete, G and de Bernard, M (2007). The neutrophil-activating protein of Helicobacter pylori (HP-NAP) as an immune modulating agent. *FEMS Immunol Med Microbiol* **50**: 157–164.
22. Amedei, A, Cappon, A, Codolo, G, Cabrelle, A, Polenghi, A, Benagiano, M *et al.* (2006). The neutrophil-activating protein of Helicobacter pylori promotes Th1 immune responses. *J Clin Invest* **116**: 1092–1101.
23. Goodwin, CS (1997). Helicobacter pylori gastritis, peptic ulcer, and gastric cancer: clinical and molecular aspects. *Clin Infect Dis* **25**: 1017–1019.
24. Fiocca, R, Villani, L, Luinetti, O, Gianatti, A, Perego, M, Alvisi, C *et al.* (1992). Helicobacter colonization and histopathological profile of chronic gastritis in patients with or without dyspepsia, mucosal erosion and peptic ulcer: a morphological approach to the study of ulcerogenesis in man. *Virchows Arch A Pathol Anat Histopathol* **420**: 489–498.
25. Dundon, WG, Nishioka, H, Polenghi, A, Papinutto, E, Zanotti, G, Montemurro, P *et al.* (2002). The neutrophil-activating protein of Helicobacter pylori. *Int J Med Microbiol* **291**: 545–550.
26. de Bernard, M and D'Elios, MM (2010). The immune modulating activity of the Helicobacter pylori HP-NAP: Friend or foe? *Toxicon* **56**: 1186–1192.
27. Yu, D, Jin, C, Leja, J, Majdalani, N, Nilsson, B, Eriksson, F *et al.* (2011). Adenovirus with hexon Tat-protein transduction domain modification exhibits increased therapeutic effect in experimental neuroblastoma and neuroendocrine tumors. *J Virol* **85**: 13114–13123.
28. Yu, D, Jin, C, Ramachandran, M, Xu, J, Nilsson, B, Korsgren, O *et al.* (2013). Adenovirus serotype 5 vectors with Tat-PTD modified hexon and serotype 35 fiber show greatly enhanced transduction capacity of primary cell cultures. *PLoS ONE* **8**: e54952.

29. Fueyo, J, Gomez-Manzano, C, Alemany, R, Lee, PS, McDonnell, TJ, Mitlianga, P *et al.* (2000). A mutant oncolytic adenovirus targeting the Rb pathway produces anti-glioma effect in vivo. *Oncogene* **19**: 2–12.
30. Guse, K, Sloniecka, M, Diaconu, I, Ottolino-Perry, K, Tang, N, Ng, C *et al.* (2010). Antiangiogenic arming of an oncolytic vaccinia virus enhances antitumor efficacy in renal cell cancer models. *J Virol* **84**: 856–866.
31. Codolo, G, Fassan, M, Munari, F, Volpe, A, Bassi, P, Rugge, M *et al.* (2012). HP-NAP inhibits the growth of bladder cancer in mice by activating a cytotoxic Th1 response. *Cancer Immunol Immunother* **61**: 31–40.
32. Iankov, ID, Allen, C, Federspiel, MJ, Myers, RM, Peng, KW, Ingle, JN *et al.* (2012). Expression of immunomodulatory neutrophil-activating protein of Helicobacter pylori enhances the antitumor activity of oncolytic measles virus. *Mol Ther* **20**: 1139–1147.
33. Iankov, ID, Blechacz, B, Liu, C, Schmeckpeper, JD, Tarara, JE, Federspiel, MJ *et al.* (2007). Infected cell carriers: a new strategy for systemic delivery of oncolytic measles viruses in cancer virotherapy. *Mol Ther* **15**: 114–122.
34. Willmon, C, Harrington, K, Kottke, T, Prestwich, R, Melcher, A and Vile, R (2009). Cell carriers for oncolytic viruses: Fed Ex for cancer therapy. *Mol Ther* **17**: 1667–1676.
35. Nakashima, H, Kaur, B and Chiocca, EA (2010). Directing systemic oncolytic viral delivery to tumors via carrier cells. *Cytokine Growth Factor Rev* **21**: 119–126.
36. Ylösmäki, E, Hakkarainen, T, Hemminki, A, Visakorpi, T, Andino, R and Saksela, K (2008). Generation of a conditionally replicating adenovirus based on targeted destruction of E1A mRNA by a cell type-specific MicroRNA. *J Virol* **82**: 11009–11015.
37. Cawood, R, Chen, HH, Carroll, F, Bazan-Peregrino, M, van Rooijen, N and Seymour, LW (2009). Use of tissue-specific microRNA to control pathology of wild-type adenovirus without attenuation of its ability to kill cancer cells. *PLoS Pathog* **5**: e1000440.
38. Leja, J, Nilsson, B, Yu, D, Gustafson, E, Akerström, G, Oberg, K *et al.* (2010). Double-detargeted oncolytic adenovirus shows replication arrest in liver cells and retains neuroendocrine cell killing ability. *PLoS ONE* **5**: e8916.
39. Polenghi, A, Bossi, F, Fischetti, F, Durigutto, P, Cabrelle, A, Tamassia, N *et al.* (2007). The neutrophil-activating protein of Helicobacter pylori crosses endothelia to promote neutrophil adhesion in vivo. *J Immunol* **178**: 1312–1320.
40. Scapini, P, Lapinet-Vera, JA, Gasperini, S, Calzetti, F, Bazzoni, F and Cassatella, MA (2000). The neutrophil as a cellular source of chemokines. *Immunol Rev* **177**: 195–203.
41. Bauerová, K and Bezek, A (1999). Role of reactive oxygen and nitrogen species in etiopathogenesis of rheumatoid arthritis. *Gen Physiol Biophys* **18** Spec No: 15–20.
42. White, E (2001). Regulation of the cell cycle and apoptosis by the oncogenes of adenovirus. *Oncogene* **20**: 7836–7846.
43. Brisslert, M, Enarsson, K, Lundin, S, Karlsson, A, Kusters, JG, Svennerholm, AM *et al.* (2005). Helicobacter pylori induce neutrophil transendothelial migration: role of the bacterial HP-NAP. *FEMS Microbiol Lett* **249**: 95–103.
44. Smart, SJ and Casale, TB (1994). TNF-alpha-induced transendothelial neutrophil migration is IL-8 dependent. *Am J Physiol* **266**(3 Pt 1): L238–L245.
45. de Jong, AL, Green, DM, Trial, JA and Birdsall, HH (1996). Focal effects of mononuclear leukocyte transendothelial migration: TNF-alpha production by migrating monocytes promotes subsequent migration of lymphocytes. *J Leukoc Biol* **60**: 129–136.
46. Del Prete, G, Chiumiento, L, Amedei, A, Piazza, M, D'Elios, MM, Codolo, G *et al.* (2008). Immunosuppression of TH2 responses in Trichinella spiralis infection by Helicobacter pylori neutrophil-activating protein. *J Allergy Clin Immunol* **122**: 908–913.e5.
47. Barash, S, Wang, W and Shi, Y (2002). Human secretory signal peptide description by hidden Markov model and generation of a strong artificial signal peptide for secreted protein expression. *Biochem Biophys Res Commun* **294**: 835–842.
48. Yu, D, Jin, C, Ramachandran, M, Xu, J, Nilsson, B, Korsgren, O, *et al.* (2012). Adenovirus serotype 5 vectors with Tat-PTD modified hexon and serotype 35 fiber show greatly enhanced transduction capacity of primary cell cultures. *PLoS One* **8**(1): e54952.
49. Danielsson, A, Dzojic, H, Nilsson, B and Essand, M (2008). Increased therapeutic efficacy of the prostate-specific oncolytic adenovirus Ad[I/PPT-E1A] by reduction of the insulator size and introduction of the full-length E3 region. *Cancer Gene Ther* **15**: 203–213.
50. Tollefson, AE, Kuppuswamy, M, Shashkova, EV, Doronin, K and Wold, WS (2007). Preparation and titration of CsCl-banded adenovirus stocks. *Methods Mol Med* **130**: 223–235.
51. O'Gorman, MR and Corrochano, V (1995). Rapid whole-blood flow cytometry assay for diagnosis of chronic granulomatous disease. *Clin Diagn Lab Immunol* **2**: 227–232.